

See discussions, stats, and author profiles for this publication at: <https://www.researchgate.net/publication/49710338>

Cross-Linked Bacterial Cellulose Networks Using Glyoxalization

ARTICLE *in* ACS APPLIED MATERIALS & INTERFACES · DECEMBER 2010

Impact Factor: 6.72 · DOI: 10.1021/am101065p · Source: PubMed

CITATIONS

13

READS

59

8 AUTHORS, INCLUDING:



[Geert Vanden Poel](#)

Royal DSM

19 PUBLICATIONS 522 CITATIONS

[SEE PROFILE](#)



[Alexander Bismarck](#)

University of Vienna

295 PUBLICATIONS 6,245 CITATIONS

[SEE PROFILE](#)



[Stephen J Eichhorn](#)

University of Exeter

114 PUBLICATIONS 4,135 CITATIONS

[SEE PROFILE](#)

Cross-Linked Bacterial Cellulose Networks Using Glyoxalization

Franck Quéro,^{†,‡} Masaya Nogi,[§] Koon-Yang Lee,[⊥] Geert Vanden Poel,[#] Alexander Bismarck,[⊥] Athanasios Mantalaris,[⊥] Hiroyuki Yano,[¶] and Stephen J. Eichhorn^{*,†,‡}

[†]Materials Science Centre, School of Materials, University of Manchester, Grosvenor Street, Manchester M13 9PL, United Kingdom

[‡]The Northwest Composite Centre, University of Manchester, Paper Science Building, Sackville Street, Manchester M13 9PL, United Kingdom

[§]Institute of Science and Industrial Research, Osaka University, Mihogaoka 8-1, Ibaraki, Osaka, 567-0047, Japan

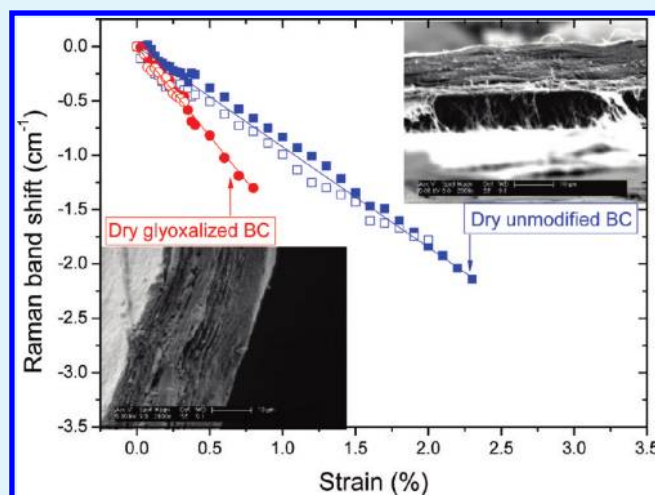
[⊥]Polymer and Composites Engineering (PaCE) Group, Department of Chemical Engineering, Imperial College London, South Kensington Campus, London SW7 2AZ, United Kingdom

[#]Thermal Analysis Group, DSM Resolve, P.O. Box 18, 6160 MD Geleen, The Netherlands

[¶]Research Institute for the Sustainable Humanosphere, Kyoto University, Uji, Kyoto 611-011, Japan

ABSTRACT: In this study, we demonstrate that bacterial cellulose (BC) networks can be cross-linked via glyoxalization. The fracture surfaces of samples show that, in the dry state, less delamination occurs for glyoxalized BC networks compared to unmodified BC networks, suggesting that covalent bond coupling between BC layers occurs during the glyoxalization process. Young's moduli of dry unmodified BC networks do not change significantly after glyoxalization. The stress and strain at failure are, however, reduced after glyoxalization. However, the wet mechanical properties of the BC networks are improved by glyoxalization. Raman spectroscopy is used to demonstrate that the stress-transfer efficiency of deformed dry and wet glyoxalized BC networks is significantly increased compared to unmodified material. This enhanced stress-transfer within the networks is shown to be a consequence of the covalent coupling induced during glyoxalization and offers a facile route for enhancing the mechanical properties of BC networks for a variety of applications.

KEYWORDS: Raman spectroscopy, bacterial cellulose, glyoxal, cross-linking, stress-transfer



INTRODUCTION

Cellulose is the most abundant and utilized polymer on earth. It is found in higher plants and, algae and is produced, under culturing conditions by bacteria, and by sea animals called tunicates.^{1,2} Bacterial cellulose (BC) is an extra-cellular product of bacteria identified for the first time by Brown.³ Several families of bacteria are cellulose producers, namely, *Acetobacter*, *Enterobacter*, *Rhizobium*, *Agrobacterium* and *Sarcina*.⁴ The acetic acid bacteria *Acetobacter xylinum* (reclassified as *Gluconacetobacter xylinum*) has been found to be one of the most productive⁵ and consequently is the most studied species. This form of BC is produced in a very pure form, since alkali treatment is performed to remove remaining proteins from bacterial cell debris. Nevertheless, contrary to cellulose from plants, BC is free of wax, hemicelluloses, and lignin.⁶

Cellulose has been found to have desirable mechanical properties and is consequently a good candidate as a reinforcement fiber in composite materials.^{7–11} In plants, it naturally plays a structural role because of its high stiffness. The crystal modulus of cellulose has been found to be ~138 GPa using X-ray diffraction^{12,13}.

More recently Young's modulus of single tunicate whiskers and BC nanofibers have been estimated using Raman spectroscopy; values of 143² and 114 GPa¹⁴ were found, respectively. A direct measurement, using an AFM cantilever method, yielded a value of 78 ± 17 GPa for BC nanofibrils.¹⁵

BC fibrous networks produced using different culturing times have been used to reinforce poly(L-lactic acid) (PLLA).¹⁶ Observations of the fracture surfaces of samples deformed in tension indicated that delamination occurred mainly between layers within the BC networks, rather than at the interface between the BC and PLLA. Consequently, before trying to improve compatibility between hydrophilic BC networks and hydrophobic PLLA through chemical modification for instance, one needs first to consolidate these networks. It was also found that the more layered the structure of these networks, the lower

Received: November 4, 2010

Accepted: December 10, 2010

the stress-transfer efficiency. Layers of BC networks have been recently reported to be weakly linked.¹⁷ Consequently in order to improve the stress-transfer efficiency of BC networks, we are aiming to cross-link the material using glyoxal. Here, we report the influence of this facile treatment on the mechanical and stress-transfer properties in both the dry and wet states.

It is possible to functionalize cellulose because of the presence of a large number of accessible hydroxyl groups along its backbone structure. These hydroxyl groups can be functionalized via esterification, polycondensation, etherification, or acetalization,^{18,19} to name a few reactions. By using an appropriate chemical substance having at least two reactive groups that can react with hydroxyl groups, covalent bonds can be formed between cellulose polymer chains, and therefore potentially between weakly linked BC layers. Several chemical substances have been reported as cross-linking agents for cellulose; namely glyoxal and its homologues, but also formaldehyde, epichlorohydrin, epoxides (1,2,3,4-diepoxybutane), dichloroethane, or diisocyanate.¹⁹ Most of these chemicals are not environmentally friendly and can be toxic. Glyoxal, however, is an almost fully biodegradable and low toxicity chemical (compared to formaldehyde) and can be obtained from renewable resources²⁰ by the oxidation of lipids and as a byproduct of biological processes.²¹ Consequently, this molecule is a good candidate for an environmentally friendly cross-linking agent for cellulose. The main application of glyoxal thus far has been in the textile industry to impart durable wet mechanical properties of cotton fabrics.²² No application of glyoxal has, to the authors' knowledge, been proposed for cross-linking BC networks. When cellulose is exposed to water, its intra- and intermolecular hydrogen bonding is disrupted, leading to a dramatic decrease of the stress-transfer and therefore mechanical properties. By cross-linking cellulose polymer chains via covalent bonds through glyoxalization, the effect of this disruption of hydrogen bonding on physical properties can be reduced. We show the potential of glyoxal to enhance the stress-transfer efficiency of BC networks, and thereby their mechanical properties. This modification is shown to persist in the wet state, and so could be used for a variety of applications; for example in composites manufacturing and biomedical applications.

EXPERIMENTAL METHODS

Materials and Chemicals. *Gluconacetobacter xylinum* (no. 13693; National Institute of Technology and Evaluation, Tokyo, Japan) and Hestrin-Schramm (HS)²³ medium were used to produce BC networks. The cells for the inoculum were cultured in test tubes statically at 27 °C for 14 days. The thick gel produced during culturing was then squeezed aseptically to remove the embedded cells. The cell suspension (25 mL) was then transferred as an inoculum for the main culture (500 mL of medium), which was incubated statically at 27 °C for 14 days. BC networks (35 mm in diameter) were purified by boiling with 2% NaOH for 2 h and then by washing with distilled water, followed by hot pressing at 2 MPa at 120 °C for 4 min to completely remove the bulk water.

Glyoxal (~40 wt % in deionized water), aluminum sulfate hexadecahydrate ($\text{Al}_2(\text{SO}_4)_3 \cdot 16 \text{H}_2\text{O}$, purity $\geq 98\%$), lithium chloride (LiCl ; $\geq 99.5\%$) and *N,N*-dimethylacetamide (DMAc; $\geq 98\%$) were purchased from Sigma-Aldrich (Gillingham, U.K.).

Glyoxal Treatment of BC Networks. A 40 mL solution containing 5 wt % glyoxal was prepared by diluting a commercial glyoxal solution (40 wt %) with deionized water. Aluminum sulfate hexadecahydrate was added with a concentration of 1 g L^{-1} to catalyze the reaction.

The solution was agitated under mechanical stirring until complete dissolution of the catalyst. Each time the glyoxalization procedure was performed, 10 narrow strips of BC ($\sim 30 \text{ mm} \times 1 \text{ mm} \times 0.06 \text{ mm}$ each) were used, corresponding to approximately 20 mg of BC in total. BC strips were immersed in the glyoxal solution for 5 h. Twenty milligram of BC immersed in a 40 mL solution containing 5 wt % glyoxal corresponds to a cellulose:glyoxal molar ratio of approximately 1:280. Glyoxal was therefore largely present in excess. During the impregnation time, the glyoxal molecules adsorbed on the surface and impregnated the structure of BC networks. These impregnated strips were then removed from the solution and placed in a convection oven at 150 °C for 15 min for glyoxalization to complete. Modified BC networks were then washed in deionized water at ~ 70 °C for 60 min. For each of these steps, deionized water was renewed. The networks were dried overnight at 110 °C.

Dissolution Test. Strips of unmodified and glyoxalized BC samples ($\sim 2.5 \text{ mm} \times 1 \text{ mm} \times 0.06 \text{ mm}$) were immersed in LiCl/DMAc (8 wt % LiCl) solution for 48 h in an environmentally controlled room at a temperature of 23 ± 1 °C and relative humidity of $50 \pm 0.5\%$. This solvent is reported to fully dissolve cellulose at room temperature.²⁴ The glyoxalized samples were weighed before and after immersion in LiCl/DMAc solution using a Mettler Toledo AB265-S/FACT version classic analytical balance. Care was taken to remove the excess of LiCl/DMAc before weighing the samples. The percentage of swelling (%) was determined after 48 h using the equation

$$\%S = \frac{W_s - W_d}{W_d} 100 \quad (1)$$

where W_s and W_d are the swollen and dry weights of the glyoxalized BC networks, respectively. Five samples were tested in total.

X-ray Diffraction. The degree of crystallinity and crystal morphology of unmodified and glyoxalized BC networks were determined using an X-ray powder diffractometer (Philips X'Pert 1) having a 1.79 Å cobalt X-ray source. Measurements were taken in the range $2\theta = 10^\circ$ to 40° using a step size of 0.04° . Five samples were analyzed for both unmodified and glyoxalized BC networks. The percentage crystallinity ($\%\chi_c$) of BC was calculated using Segal's method²⁵ and is defined as

$$\%\chi_c = \frac{I_{200} - I_{\text{amorphous}}}{I_{200}} 100 \quad (2)$$

where I_{200} is the intensity of the 200 reflection plane and $I_{\text{amorphous}}$ is the intensity of the amorphous phase at 18° , if a copper X-ray source is used. For a cobalt source the intensity at 21° is recorded. Consequently the 200 reflection plane is positioned at 27° . For the lateral crystal size ($L_{(200)}$) determination, Scherrer's equation was used, namely

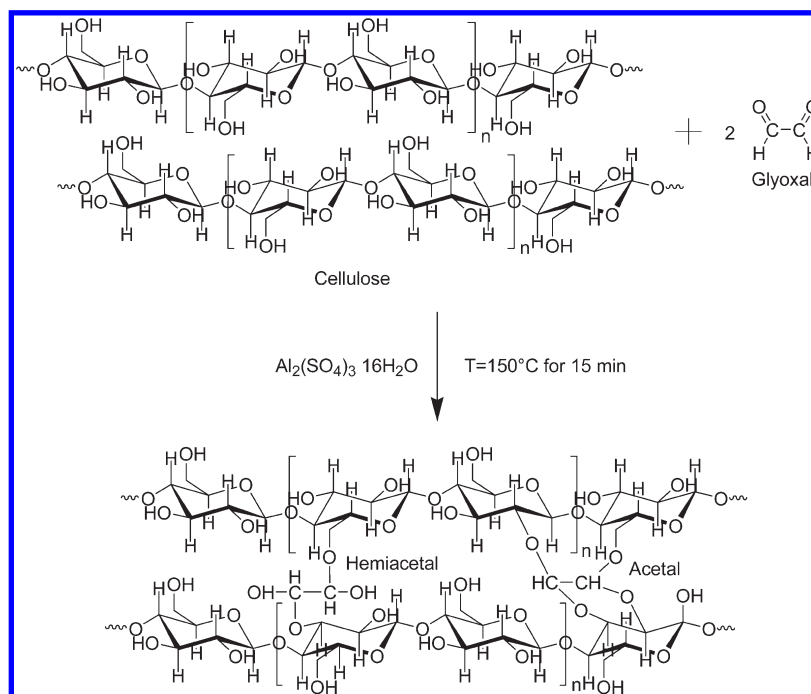
$$L_{(200)} = \frac{K\lambda}{\beta \cos \theta} \quad (3)$$

where β is the full width at half-maximum of the 200 reflection, θ is the Bragg angle, and a value of $K = 0.91$ was used.

Thermogravimetric Analysis. The thermal degradation behavior of unmodified and glyoxalized BC was investigated using thermogravimetric analysis (TGA Netzsch TG 209 F1). The samples (approximately 5 mg) were heated from 25 to 600 °C at a heating rate of $5^\circ \text{C min}^{-1}$ under a flow of 30 mL min^{-1} nitrogen purge gas. Experiments were repeated three times to ensure repeatability. The onset and degradation temperatures were obtained from the first derivative of the loss weight as a function of temperature. The temperature control in the furnace was ± 1 °C and the samples were conditioned under ambient temperature and humidity prior to testing.

Water/Air Contact Angle Measurements. Advancing θ_a and receding θ_r contact angles were measured on unmodified and glyoxalized BC networks using a sessile drop method (DSA 10 Mk 2, Krüss

Scheme 1. Cross-Linking Reaction between Cellulose and Glyoxal with the Formation of Hemiacetal and Acetal Linkages



GmbH, Hamburg, D) at 20°C . Droplets of approximately $20\ \mu\text{L}$ of ultra pure water were placed on the surface of unmodified and glyoxalized BC networks using a motorized syringe and the drop volume was increased at a rate of $6.32\ \mu\text{L}\ \text{min}^{-1}$. Images of these sessile drops were processed using DSA software version 1.80.1.12. A single contact angle measurement took approximately 4 min to try to limit unavoidable capillarity and absorption effects on such hydrophilic materials. Measurements were repeated on 5 different positions on the samples.

Zeta-Potential Measurements. The zeta (ζ)-potentials of unmodified and glyoxalized BC were measured using an electrokinetic analyzer (EKA, Anton Paar, Graz, Austria) based on a streaming potential method. To exclude any overlaying effects due to the swelling of unmodified and glyoxalized BC networks or the extraction of water-soluble components, the pH-dependent ζ -potentials were measured after a time dependent measurement was taken. During the time-dependent measurements, the samples were equilibrated in 1 mM KCl electrolyte solution by means of a single long time ζ -potential measurement at 20°C . The swelling behavior of the (modified) bacterial cellulose was determined from the kinetic parameters ζ_0 (initial ζ -potential at first contact with water) and ζ_∞ (final ζ -potential, asymptotic approach). The relative change in ζ -potential was found using the equation

$$\Delta\zeta = \frac{\zeta_0 - \zeta_\infty}{\zeta_0} \quad (4)$$

It has been shown that this quotient is proportional to the water uptake at 100% relative humidity (the sorption capacity) of natural fibers.²⁶ A pH-dependent ζ -potential measurement was then conducted by changing the pH of the electrolyte solution via the titration of 0.1 N HCl or KOH, using a titration unit (RTU, Anton Paar, Graz, Austria).

Relative Water Absorption Capacity. Unmodified and glyoxalized BC networks ($\sim 5\ \text{mm} \times 1\ \text{mm} \times 0.06\ \text{mm}$) were conditioned for 7 days at $23 \pm 1^\circ\text{C}$ and a relative humidity of $50 \pm 0.5\%$ and immersed in deionised water for 48 h. The samples were weighed after 2, 5, 11, 24, and 48 h using a top pan balance. Care was taken to remove excess water

using absorbent paper before weighing the samples. Relative water absorption capacity (%RWAC) was determined using the equation

$$\%RWAC = \frac{w_t - w_{t0}}{w_{t0}} 100 \quad (5)$$

where w_{t0} and w_t are the weights of the samples before and after water immersion, respectively. Five samples were tested for each material.

Mechanical Properties. Unmodified and glyoxalized BC strips ($\sim 20\ \text{mm} \times 1\ \text{mm} \times 0.06\ \text{mm}$) were secured to 20 mm gauge length testing cards using a two-part cold curing epoxy resin (Araldite). Tensile tests were conducted using a tensile testing machine (Instron 2511-111, High Wycombe, U.K.). The full-scale load and the crosshead speed used were 50 N and $0.5\ \text{mm}\ \text{min}^{-1}$, respectively. The machine compliance was determined and found to be $4.42 \times 10^{-3}\ \text{mm}\ \text{N}^{-1}$. Dry and wet mechanical tests were conducted at $23 \pm 1^\circ\text{C}$ and a relative humidity of $50 \pm 0.5\%$. The samples were preconditioned under the same environmental conditions for 24 h prior to testing. A total of 10 samples were tested for each material. Sample widths and thicknesses were determined using an optical microscope and a micrometer, respectively.

For wet mechanical properties determination, unmodified and glyoxalized BC networks were immersed in deionised water for 48 h at $23 \pm 1^\circ\text{C}$. The samples were then removed from the water and secured on paper testing cards using cyanoacrylate glue (Sigma Aldrich, Gillingham, UK).

The fracture surfaces of dry and wet unmodified and glyoxalized BC networks deformed in tension were observed using a scanning electron microscope (Phillips XL-30 FEG-SEM). The acceleration voltage used was 5 kV. Prior to SEM imaging, the samples were fixed onto metal stubs using carbon tabs and gold coated at 40 mA for 2 min.

Raman Spectroscopy. In order to follow the molecular deformation of unmodified and glyoxalized BC networks a Raman spectrometer (Renishaw system-1000, Wotton-under-Edge, U.K.) coupled with an optical microscope and a near-infrared laser (785 nm) was used. The laser was focused to a $1\text{--}2\ \mu\text{m}$ spot using a $\times 50$ magnification long working distance lens. Dry unmodified and glyoxalized BC strips were

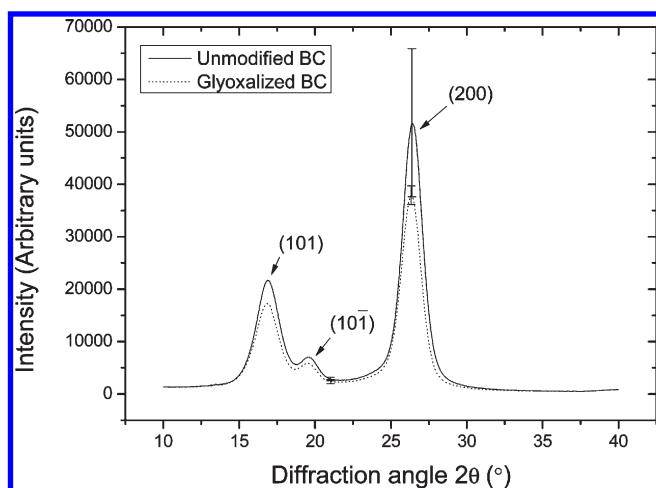


Figure 1. Average X-ray diffraction patterns for dry unmodified and glyoxalized BC networks with (200), (101), and (101̄) diffraction planes labelled. Error bars at 21° and at the maximum of the 200 orientation plane represent standard deviations for 5 samples.

mounted on paper testing cards using a two-part cold-curing epoxy resin (Araldite, Huntsman, U.K.). The samples were deformed in tension using a customized deformation rig (Deben Microtest, Deben, Bury St Edmonds, UK). The compliance of the deformation rig was determined to be $3.14 \times 10^{-4} \text{ mm N}^{-1}$. The gauge length of the samples and the full scale of the load cell used were 20 mm and 2 kN, respectively. During the deformation, the strain was increased incrementally by 0.025% and then 0.1% at an elongation rate of $0.033 \text{ mm min}^{-1}$. A Raman spectrum was recorded at each increment using an exposure time of 30 s and 4 accumulations. The peak positions of the Raman band initially located at approximately 1095 cm^{-1} were fitted using a mixed Gaussian/Lorentzian function and an algorithm suggested by Marquardt.²⁷ Experiments were repeated 2 times for unmodified and glyoxalized BC networks. Unmodified BC networks were also submitted to the exact same conditions as for glyoxal treatment, except that no glyoxal was used. These samples are referred to as “thermally treated”. The molecular deformation of these materials was followed as well. Two samples were tested for reproducibility.

Molecular deformation of samples in the wet state was also investigated. Unmodified and glyoxalized BC networks were immersed in deionized water for 48 h. The samples were then removed from the water and secured on paper testing cards using cyanoacrylate glue. During sample preparation and molecular deformation, the BC networks were regularly wetted. Two samples were tested for each material.

RESULTS AND DISCUSSION

Scheme 1 reports the chemical reaction occurring between glyoxal and cellulose. The former can react with the hydroxyl groups of cellulose either by an acetalization reaction or by glyoxalization.²⁸ They can form either or both acetal and hemeacetal linkages during the curing process.²⁹ Aluminum salts were found to be helpful to catalyze the cross-linking of cellulose.^{30,22,31} Meyer et al. described the mechanism of catalysts to cross-link cotton with formaldehyde.³² This mechanism is based on a proton-catalyzed acetal formation.³¹ To check whether the cellulose was cross-linked, we immersed unmodified and glyoxalized samples in LiCl/DMAc for 48 h. Unmodified BC samples were found to fully dissolve after 24 h, whereas glyoxalized BC samples did not dissolve, but remained in a swollen state. After 48 h, the percentage of swelling was found to be $30 \pm 4\%$. Even after 2 months, glyoxalized BC

Table 1. Percentage Crystallinity (χ_c) and Lateral Crystal Sizes (L) for Dried Unmodified and Glyoxalized BC Networks

material	χ_c (%)	L (200) (Å)
unmodified BC	94.3 ± 1.2	63.0 ± 2.1
glyoxalized BC	93.9 ± 0.2	63.6 ± 0.5

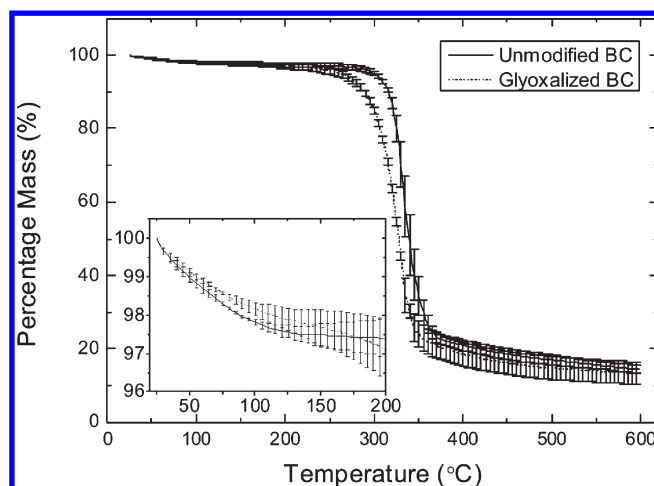


Figure 2. Typical thermal degradation profiles for unmodified and glyoxalized BC networks. Error bars are standard deviations from the mean. The insert represents the thermal behavior from 25 to 200 °C.

Table 2. Onset and Peak Degradation Temperatures for Unmodified and Glyoxalized BC Networks

material	onset degradation temperature (°C)	peak degradation temperature (°C)
unmodified BC	319 ± 1	335 ± 4
glyoxalized BC	299 ± 1	330 ± 3

networks were still not dissolved. Consequently, it is very likely that cross-linking occurred between the BC fibrils and layers. A dissolution method has already been used to assess the extent of cross-linking in chemically modified cotton, with cuprammonium hydroxide as a solvent.³³

Figure 1 reports average X-ray diffraction patterns for dry unmodified and glyoxalized BC networks. It can be seen that the crystal structure is unchanged after glyoxalization because (101), (101̄), and (200) diffraction planes are still observed. Table 1 reports percentage crystallinity values and crystal dimensions for dry unmodified and glyoxalized BC networks. No significant difference between dry unmodified and glyoxalized BC networks is observed. This result suggests that cross-linking is likely to occur only at the surface of BC fibrils and in amorphous regions, meaning that heterogeneous modification of BC has occurred. Hydroxyl groups located inside crystal regions are believed to be inaccessible to chemical modification.³⁴

Figure 2 reports the thermal degradation behavior for unmodified and glyoxalized BC networks. An initial weight loss, due to drying water, was observed in the temperature range of 0 to 200 °C. No significant differences between unmodified and glyoxalized BC networks were observed in this region. This indicates that there is no difference in moisture content between these samples (see insert to Figure 2). This means that if a change of mechanical or stress-transfer properties is observed in the dry state, it should

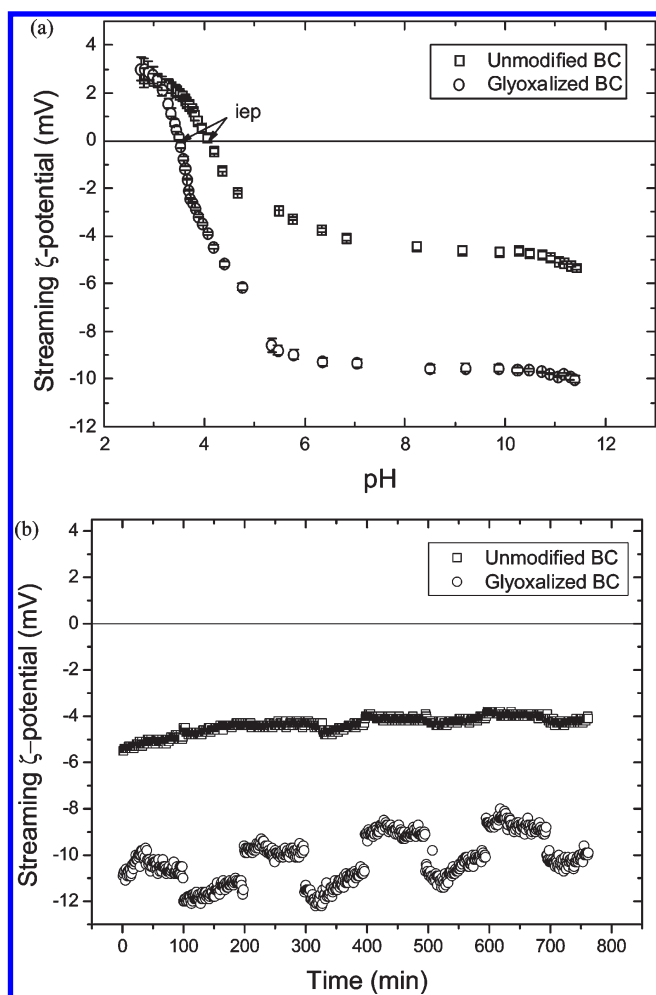


Figure 3. (a) Streaming zeta-potentials of unmodified and glyoxalized BC as a function of pH; (b) streaming zeta-potentials of unmodified and glyoxalized BC as a function of time.

be due to only the presence of cross-linking, and not from a plasticization effect due to the presence of moisture. A second weight loss is visible from 200 to 375 °C, which is attributed to the degradation of cellulose. Table 2 reports the onset and peak degradation temperatures for unmodified and glyoxalized BC networks. In agreement with previous reports,^{35,36} there is only a slight decrease in the onset degradation temperatures after glyoxalization, meaning that this process does not dramatically decrease the thermal stability of BC.

Glyoxal has been previously found to be useful to hydrophobize chitosan.³⁷ This suggests that it ought to be possible to also render BC networks hydrophobic. To test this hypothesis, water/air contact angle measurements on BC films were conducted. However, one should note that the measured contact angles are not thermodynamic contact angles as the values are influenced by the wetting behavior of the cellulose fibrils and the imbibition into the paperlike sheet. The advancing contact angles were found to be $17.4 \pm 1.7^\circ$ and $29.6 \pm 1.8^\circ$ for unmodified and glyoxalized BC networks, respectively. Because of the extreme hydrophilicity of BC, it was impossible to measure the receding contact angle for unmodified BC. However, the receding contact angle for glyoxalized BC networks was $9.9 \pm 0.6^\circ$. These results suggest a mild increase in the hydrophobicity of the BC networks, but not to the same extent as seen for chitosan.³⁷

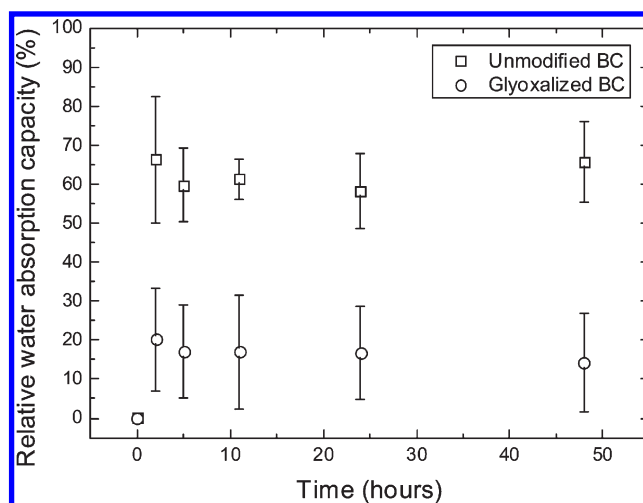


Figure 4. Relative water absorption as a function of time for unmodified and glyoxalized BC.

Figure 3 shows the ζ -potentials, measured using the streaming potential method, of unmodified and glyoxalized BC networks as a function of pH. The negative ζ -potential plateau (ζ_{plateau}) and isoelectric point (iep) in the acidic pH range indicate that the surface of unmodified and glyoxalized BC networks contain acidic surface functional groups. The shift in the iep of glyoxalized BC to lower pH confirms that the glyoxalization reaction introduces more free acidic functional groups to the surface. We also calculated $\Delta\zeta$ from $\zeta = f(t)$ for unmodified and glyoxalized BC networks (see Figure 3b). Values of 0.255 and 0.184 were found for unmodified BC and glyoxalized BC, respectively. The higher value of $\Delta\zeta$ indicates that unmodified BC networks have a higher relative water absorption capacity as compared to glyoxalized BC networks. This is not surprising because of the hydrophilic nature of unmodified BC.

Figure 4 reports relative water absorption as a function of time for unmodified BC and glyoxalized BC. We use the word “relative” because these results are relative to the moisture content at 23 °C and 50% relative humidity. After 2 h, unmodified and glyoxalized BC networks were saturated with water; no significant changes were observed after 5, 12, 24, and 48 h. A significant difference between the relative water absorption capacities of unmodified and glyoxalized BC networks is however noted. This result is consistent with the trend observed from the time depended ζ -potentials (the smaller $\Delta\zeta$, the lower the relative water absorption capacity) and with the contact angle and ζ -potential measurements because a more hydrophobic surface will absorb less water than a more hydrophilic one. Hence the presence of cross-linking must also reduce the swelling of BC networks with water. This reduced relative water absorption capacity has also been observed for biodegradable plastics made from soy bean products cross-linked with glyoxal.³⁷ This difference in relative water absorption capacity will have to be taken into account when interpreting the stress-transfer and mechanical properties in the wet state. This result is also interesting because moisture/swelling resistance is often an issue for cellulose-based biocomposites. The use of glyoxalized BC networks could therefore help to produce biocomposites with enhanced moisture/swelling resistance.

Images a and b in Figure 5 show scanning electron microscopy images of the fracture surfaces of dry unmodified and glyoxalized BC networks deformed in tension. Clear delamination of BC layers

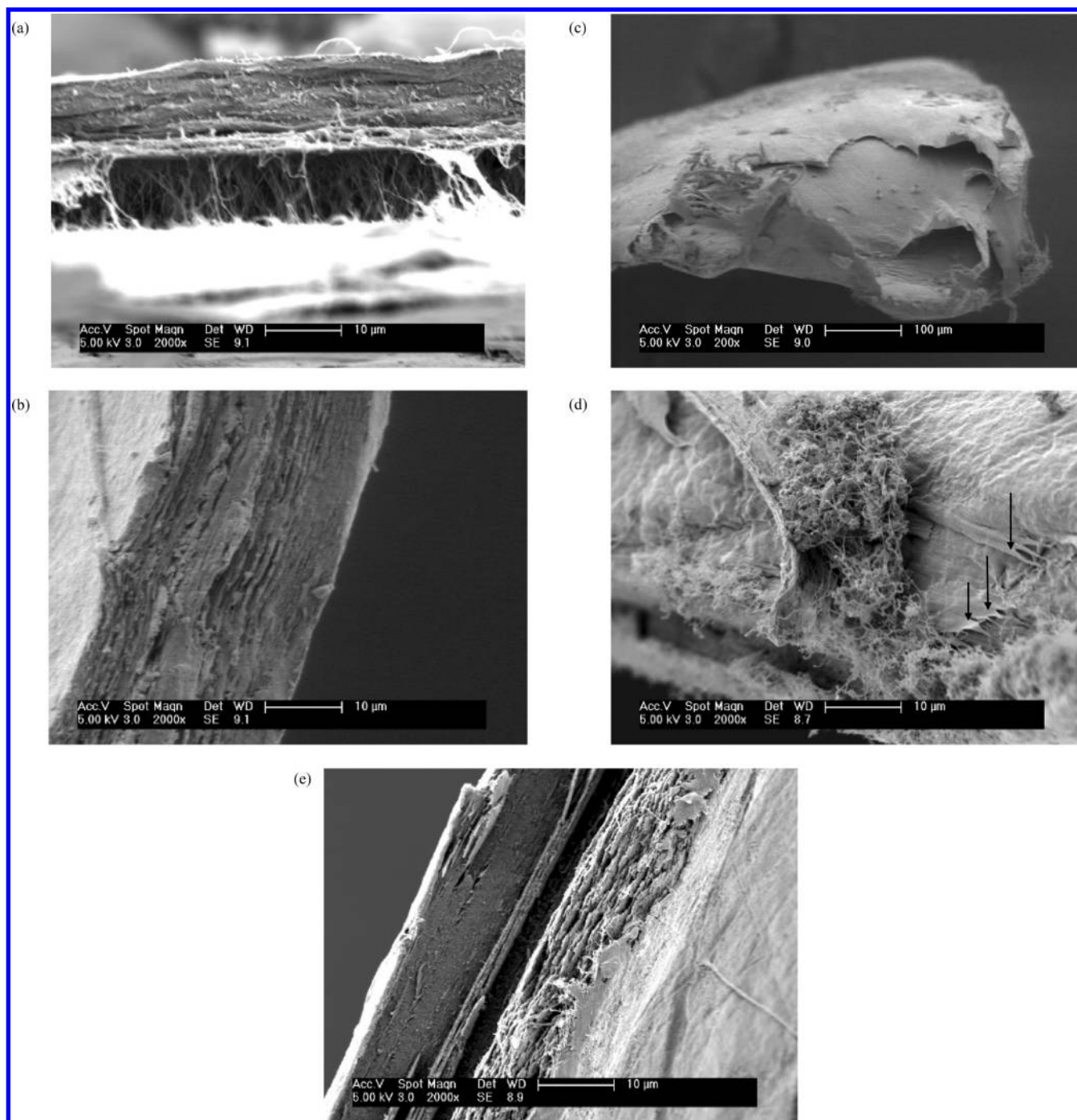


Figure 5. Scanning electron microscope images of fracture surfaces for dry (a) unmodified and (b) glyoxalized BC networks and for wet (c) unmodified and (e) glyoxalized BC networks. Image d presents a longitudinal observation in the tensile direction for wet unmodified BC networks.

is observed for the unmodified networks. BC fibrils can also be seen bridging these delaminated layers which must play a role in the fracture process. Such a delamination process does not occur for dry glyoxalized BC networks, which must be due to the presence of chemical cross-linking between layers. Figure 5c reports scanning electron microscope images for unmodified BC samples fractured while wet (the samples are dry within the vacuum chamber of the SEM). The cross-sections of the samples appear to be considerably reduced compared to the dry samples and delamination of the layers has occurred. Figure 5d presents a SEM image for the same material in the longitudinal direction

(tensile direction) showing some kind of plastification effect (see arrows). Figure 5e shows a SEM image for the tensile fracture surface of a wet glyoxalized BC network. These samples were found to maintain their dimensions, not reducing in thickness. Delamination of BC layers is however observed for this sample (dark central region) but not to the same extent as observed for dry unmodified BC networks.

Figure 6 reports typical stress–strain curves for dry and wet unmodified and glyoxalized BC networks as well as for “thermally treated” dry unmodified BC networks. The mechanical properties of dry unmodified and glyoxalized BC networks are also reported

in Table 3. We also report the mechanical properties for “thermally treated” dry unmodified BC networks. In the dry state, one can clearly see that glyoxalization of the samples reduces stress and strain at failure and the work of fracture, indicating an embrittlement of the material. Indeed this embrittlement is matched by the clean fracture surfaces observed for glyoxalized BC networks (see Figure 5b). This embrittlement may occur due to the presence of cross-linking between BC layers, which will reduce layer-to-layer mobility and consequently delamination. Cross-linking must also occur in the plane of the specimen, which could reduce orientation effects previously reported for BC networks.³⁸ No difference between Young's modulus of unmodified and glyoxalized BC networks was observed. Parts of the glyoxalization procedure itself (without the presence of glyoxal) may be responsible for this result. Consequently, we investigated the impact of this treatment on the mechanical properties of dry BC networks, which might reduce the level of hydrogen bonding. To answer that question, we submitted BC networks to the same conditions as for the glyoxalization treatment, except that no glyoxal was used, and we determined the tensile mechanical properties of the resulting specimens. The data are reported in Table 3, and are referred as “thermally treated”. Comparing the mechanical properties for dry unmodified BC networks and the “thermally treated” samples, a decrease of 23% in Young's modulus is observed. Stress, strain at failure, and work of fracture do not significantly change. This clearly indicates that a part of the glyoxalization process, possibly the thermal treatment, induces a reduction in Young's modulus of the samples, which may be related to a reduction of hydrogen bonding. For further investigation, Raman spectroscopy has been used to study the influence of

the glyoxalization process on the molecular deformation, but this will be described later in this article. Another reason for Young's modulus of glyoxalized BC networks not being significantly higher than unmodified BC networks is that some glyoxal molecules may have partially reacted with cellulose, as suggested by zeta-potential measurements. This means that the amount of available hydroxyl groups may decrease, and since the latter are involved in hydrogen bonding, this might further explain why Young's modulus was not significantly increased after glyoxalization.

When the BC networks are in the wet state, a large decrease in Young's modulus and stress at failure occurs. An increase in the strain to failure for wet unmodified BC networks compared to dry unmodified BC networks was also observed. Young's modulus, stress at failure, and strain to failure change by 438, 1570, and 261%, respectively, when samples are in the wet state. These significant changes could be explained by the disruption of intermolecular hydrogen bonding by competitive binding of water molecules, allowing slippage between BC fibrils. A disruption of intramolecular hydrogen bonding of BC nanofibrils can also be expected along with a reduction of van der Waals interactions between BC layers. The modulus of wet glyoxalized BC networks is reduced by 77%, compared to the dry state. The stress at failure does not change significantly, but the strain to failure is increased by 137%. The presence of cross-links that prevent cellulose polymer chains from slipping from one another is therefore thought to maintain the strength of the networks. This is also supported by work of fracture values shown in Table 3. Wet glyoxalized BC networks have a lower value of work of fracture ($1.3 \pm 0.8 \text{ MJ m}^{-3}$) compared to wet BC networks ($5.2 \pm 0.6 \text{ MJ m}^{-3}$) meaning that cross-links may limit layer-to-layer and nanofiber-to-nanofiber mobility even if intermolecular hydrogen bonding is disrupted.

Figure 7a reports typical Raman spectra for unmodified and glyoxalized BC networks. We did not observe any difference between the Raman spectra, which suggests that the cellulose backbone has not been affected by chemical modification. This also confirms that heterogeneous modification has occurred as previously suggested by X-ray diffraction. However the whole spectrum from unmodified BC has a higher intensity compared to glyoxalized BC. This may be due to the presence of the excess of glyoxal introduced during the glyoxalization treatment. The Raman band initially located at 1095 cm^{-1} , highlighted in Figure 7a, has been extensively used for stress-transfer quantification in cellulose materials.^{39–44} This band is thought to be representative of C–O ring stretching modes⁴⁵ and/or the C–O–C glycosidic bond stretching.^{43,46} Figure 7b and 7c report typical shifts in the position of the Raman band initially located at 1095 cm^{-1} for dry unmodified and glyoxalized BC networks, respectively. It was noted that the shift in this band is higher in magnitude for dry networks compared to wet samples, in agreement with previous work on wet cellulose nanowhiskered composite materials.⁴¹ As previously mentioned earlier, we

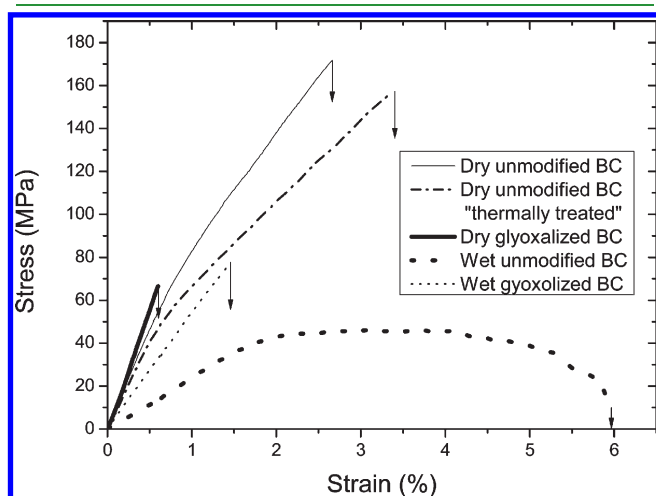


Figure 6. Typical stress–strain curves for dry and wet unmodified and glyoxalized BC networks.

Table 3. Mechanical Properties for Dry and Wet Unmodified and Glyoxalized BC Networks^a

material	E (GPa)	σ_f (MPa)	ϵ_f (%)	G (MJ m^{-3})
dry unmodified BC	10.1 ± 1.5	165.1 ± 33.9	2.6 ± 0.6	2.5 ± 0.9
dry unmodified BC (thermally treated)	7.8 ± 1.1	180.1 ± 24.2	3.6 ± 0.4	3.7 ± 0.8
dry glyoxalized BC	10.7 ± 1.4	71.1 ± 36.1	0.6 ± 0.3	0.3 ± 0.2
wet unmodified BC	1.9 ± 0.2	9.9 ± 1.5	9.3 ± 1.9	5.2 ± 0.6
wet glyoxalized BC	6.1 ± 1.4	76.8 ± 21.2	1.5 ± 0.7	1.3 ± 0.8

^a E , Young's modulus; σ_f , stress at failure; ϵ_f , strain at failure; and G , work-of-fracture.

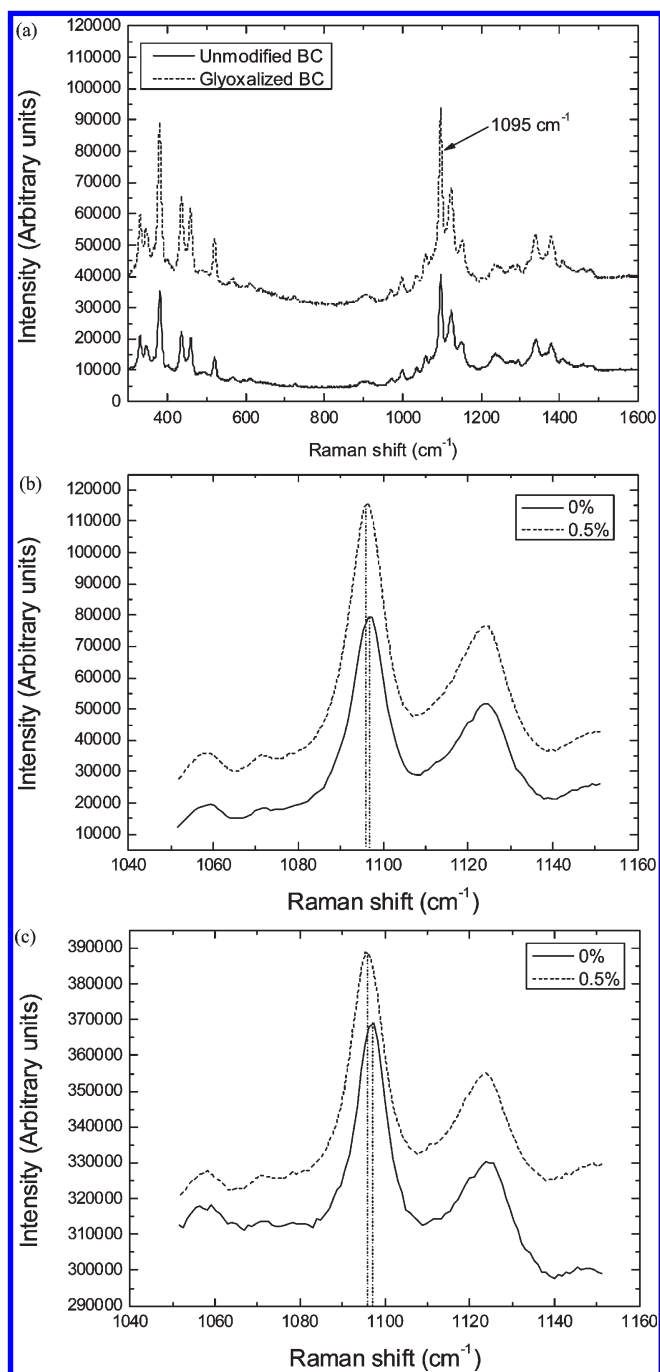


Figure 7. (a) Typical Raman spectra for dry unmodified and glyoxalized BC networks; Typical shifts in the position of the Raman band initially located at 1095 cm^{-1} toward a lower wavenumber for a dry (b) unmodified BC network and (c) a glyoxalized BC network. Percentage values correspond to the level of tensile deformation.

also investigated the influence of parts of the glyoxalization treatment, excluding the presence of glyoxal itself, on the molecular deformation of BC networks. Figure 8a reports the shift in the position of the Raman band initially located at 1095 cm^{-1} as a function of tensile deformation for dry unmodified “thermally treated” and unmodified BC networks. The term “thermally treated” refers to BC networks submitted to the same treatment as for glyoxalized BC networks without the presence of glyoxal. One can clearly see that “thermally treated” BC networks have a lower

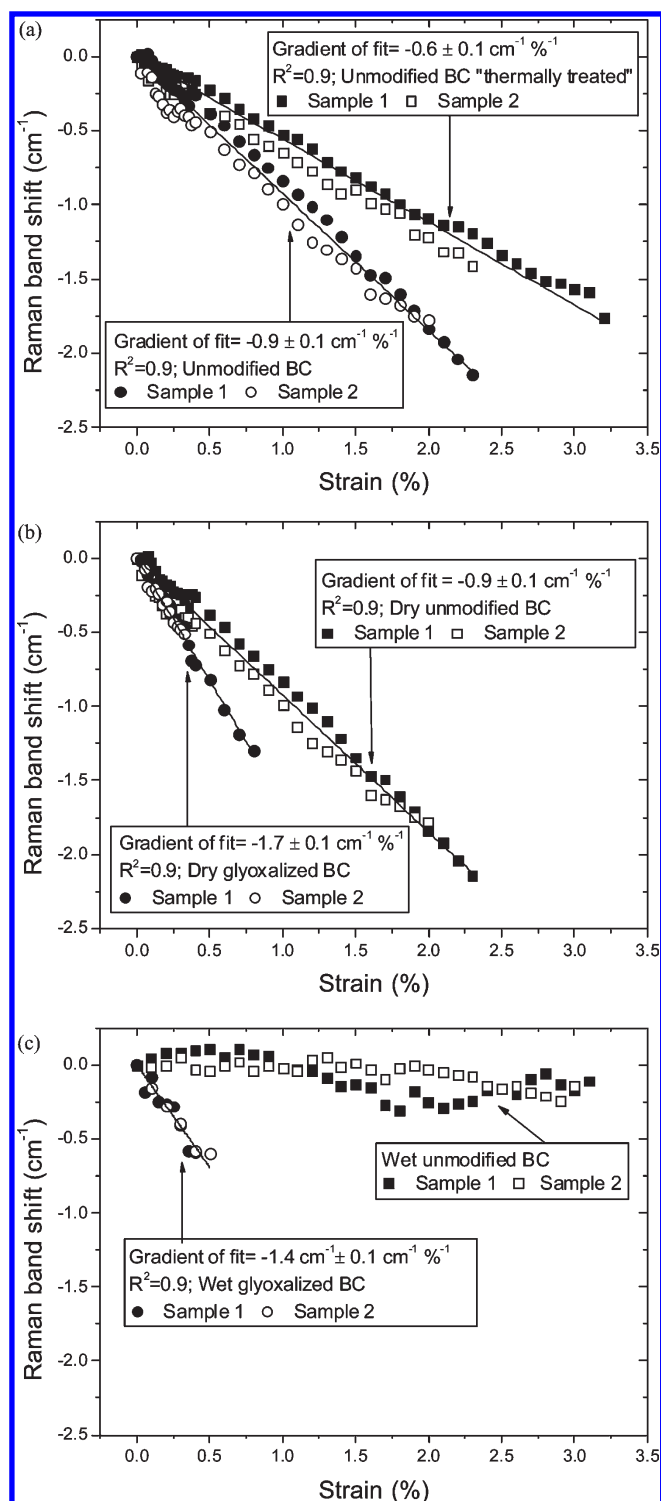


Figure 8. Detailed typical shifts in the position of the Raman band located at 1095 cm^{-1} for (a) dry unmodified “thermally treated” and unmodified BC networks, (b) dry unmodified and glyoxalized BC networks, and (c) wet unmodified and glyoxalized BC networks. Gradients are the slopes of the linear regressions applied to the data. The black and white symbols represent two independent measurements from two different samples.

stress-transfer efficiency ($-0.6 \pm 0.1\text{ cm}^{-1}\text{ \%}^{-1}$) compared to unmodified BC networks ($-0.9 \pm 0.1\text{ cm}^{-1}\text{ \%}^{-1}$). This shows that the conditions of glyoxal treatment affect the stress-transfer properties of the networks. A possible reduction of the level of

inter and intramolecular hydrogen bonding may result in a lower level of molecular deformation. This result is in accordance with Young's modulus data reported in Table 3. Figure 8b reports the detailed typical shifts in the position of the Raman band initially located at 1095 cm^{-1} as a function of strain for dry unmodified and glyoxalized BC networks. The stress-transfer efficiency of the networks can be obtained from the gradient of a linear fit to these data. Higher stress-transfer efficiency is observed for glyoxalized BC networks compared to unmodified samples, which is an indication of the cross-linking that has taken place. The gradient of these linear fits for dry unmodified and glyoxalized BC networks were $-0.9 \pm 0.1\text{ cm}^{-1}\text{ \%}^{-1}$ and $-1.7 \pm 0.1\text{ cm}^{-1}\text{ \%}^{-1}$, respectively. As previously noted, less delamination occurred for glyoxalized BC networks, which is thought to contribute to the higher stress-transfer efficiency. As a consequence of this, less energy is likely to be dissipated throughout the structure. This is confirmed by the higher work of fracture for dry unmodified BC networks compared to glyoxalized BC networks (Table 3).

Figure 8c reports the stress-transfer properties of the wet BC networks, as revealed by the shift in the position of the Raman band located at 1095 cm^{-1} . It is clear that the presence of water within unmodified BC networks almost completely suppresses their stress-transfer efficiency. This effect has also been observed for cellulose whisker-based nanocomposites exposed to water.⁴¹ This suggests that water has fully penetrated the BC networks and, therefore, acts as a plasticizer, disrupting hydrogen bonding between fibrils, and consequently reducing local molecular deformation and therefore stress-transfer within the network. The stress-transfer efficiency of wet glyoxalized BC networks is however preserved by cross-linking; the linear fit to these data was found to be $1.4 \pm 0.1\text{ cm}^{-1}\text{ \%}^{-1}$, which is only slightly lower than for dry glyoxalized BC networks ($1.7 \pm 0.1\text{ cm}^{-1}\text{ \%}^{-1}$). This explains why the mechanical properties of glyoxalized BC networks, particularly strength, were hardly affected by the presence of water (see Table 3). Differences in the stress-transfer efficiencies of dry and wet glyoxalized BC networks must be due to the removal of hydrogen bonding after immersion in water. Water absorption experiments showed that glyoxalized BC networks absorb much less water than unmodified BC networks, and so this might also explain why stress-transfer is preserved for wet glyoxalized BC networks.

CONCLUSIONS

This study has shown that it is possible to cross-link BC networks via glyoxalization. The glyoxalization process was found to not significantly change the degree of crystallinity and crystal morphology of the BC, meaning that heterogeneous modification of cellulose occurred. Thermogravimetric analysis showed that the onset and peak degradation temperatures were significantly reduced after glyoxalization. Contact angle and ζ -potential measurements showed that glyoxal rendered the BC networks hydrophobic. In the dry state, Young's modulus was found not to be significantly changed after glyoxalization. Stress and strain at failure, and work of fracture, however, were found to reduce upon modification. The reduced work of fracture values were supported by tensile fracture surface observations using scanning electron microscopy, suggesting that delamination of the layered structure of glyoxalized BC networks also reduced, because of the presence of cross-linking. In the wet state, the mechanical properties of unmodified BC networks were reduced due to the disruption

of hydrogen bonding. The mechanical properties, particularly the strength, of wet glyoxalized BC networks did not however reduce, compared to the dry state, again due to the presence of cross-linking. This was also supported by scanning electron microscopy imaging. Consequently, glyoxal cross-linking offers dimensional and mechanical stability to the BC networks when exposed to moisture. Relative water absorption capacity experiments clearly showed that glyoxalized BC networks do not absorb as much water as unmodified BC networks. ζ -potential measurements also confirmed this result. These findings could have implications for the design of biocomposites generated from BC with increased moisture resistance. Finally, Raman spectroscopy revealed the stress-transfer mechanisms of unmodified and glyoxalized BC networks both in the dry and wet states. Micro-mechanical characterization showed that glyoxalization of BC networks results in a higher stress-transfer efficiency. This was found to be also true in the wet state. This greater stress-transfer efficiency of glyoxalized BC networks is thought to be due to the presence of cross-linking, but also to difference in the relative water absorptions of the networks. The use of glyoxal therefore provides a facile approach to modify the stress-transfer properties of BC networks, which could be used for a range of applications.

AUTHOR INFORMATION

Corresponding Author

*s.j.eichhorn@manchester.ac.uk. Telephone: +44 (0)161 306 5982. Fax: +44 (0)161 306 3586.

ACKNOWLEDGMENT

The authors thank the EPSRC for funding the PhD studentships for F.Q. and K.Y.L. under Grant GR/F028946 and EP/F032005/1. Thanks are extended to Dr. Henning Althoefer from BASF for useful advice.

REFERENCES

- (1) Ranby, B. G. *Ark. Kemi* **1952**, *4*, 241–248.
- (2) Sturcova, A.; Davies, G. R.; Eichhorn, S. J. *Biomacromolecules* **2005**, *6*, 1055–1061.
- (3) Brown, A. J. J. *Chem. Soci.* **1886**, *49*, 432–439.
- (4) Jonas, R.; Farah, L. F. *Polym. Degrad. Stab.* **1998**, *59*, 101–106.
- (5) Keshk, S.; Razek, T. M. A.; Sameshima, K. *Afr. J. Biotechnol.* **2006**, *5*, 1519–1523.
- (6) Nishi, Y.; Uryu, M.; Yamanaka, S.; Watanabe, K.; Kitamura, N.; Iguchi, M.; Mitsunashi, S. *J. Mater. Sci.* **1990**, *25*, 2997–3001.
- (7) Kim, Y.; Jung, R.; Kim, H. S.; Jin, H. J. *Curr. Appl. Phys.* **2009**, *9*, S69–S71.
- (8) Gindl, W.; Keckes, J. *Compos. Sci. Technol.* **2004**, *64*, 2407–2413.
- (9) Yano, H.; Sugiyama, J.; Nakagaito, A. N.; Nogi, M.; Matsuura, T.; Hikita, M.; Handa, K. *Adv. Mater.* **2005**, *17*, 153–155.
- (10) Gea, S.; Torres, F. G.; Troncoso, O. P.; Reynolds, C. T.; Vilasecca, F.; Iguchi, M.; Peijs, T. *Int. Polym. Process.* **2007**, *22*, 497–501.
- (11) Lee, K. Y.; Blaker, J. J.; Bismarck, A. *Compos. Sci. Technol.* **2009**, *69*, 2724–2733.
- (12) Sakurada, I.; Nukushina, Y.; Ito, T. *J. Polym. Sci.* **1962**, *57*, 651–660.
- (13) Nishino, T.; Takano, K.; Nakamae, K. *J. Polym. Sci., Part B* **1995**, *33*, 1647–1651.
- (14) Hsieh, Y.-C.; Yano, H.; Nogi, M.; Eichhorn, S. J. *Cellulose* **2008**, *15*, S07–S13.
- (15) Guhados, G.; Wan, W. K.; Hutter, J. L. *Langmuir* **2005**, *21*, 6642–6646.
- (16) Quero, F.; Nogi, M.; Yano, H.; Abdulsalami, K.; Holmes, S. M.; Sakakini, B. H.; Eichhorn, S. J. *ACS Appl. Mater. Interfaces* **2010**, *2*, 321–330.

- (17) Nogi, M.; Yano, H. *Adv. Mater.* **2008**, *20*, 1849–1852.
- (18) Heinze, T.; Liebert, T. *Prog. Polym. Sci.* **2001**, *26*, 1689–1762.
- (19) Klemm, D.; Philipp, B.; Heinze, T.; Heinze, U.; Wagenknecht, W., *Comprehensive Cellulose Chemistry: General Principles and Analytical Methods*; Wiley-VCH: Weinheim, Germany, 1998; Vol. 1.
- (20) Ramires, E. C.; Megiatto, J. D.; Gardrat, C.; Castellan, A.; Frollini, E. *Polimeros* **2010**, *20*, 126–133.
- (21) Miyata, T.; Kurokawa, K.; De Strihou, C. V. *J. Am. Soc. Nephrol.* **2000**, *11*, 1744–1752.
- (22) Welch, C. M.; Danna, G. F. *Text. Res. J.* **1982**, *52*, 149–157.
- (23) Hestrin, S.; Schramm, M. *Biochem. J.* **1954**, *58*, 345–352.
- (24) McCormick, C. L.; Callais, P. A.; Hutchinson, B. H. *Macromolecules* **1985**, *18*, 23942401.
- (25) Segal, L.; Creely, J. J.; Martin, A. E.; Conrad, C. M. *Text. Res. J.* **1959**, *29*, 786–794.
- (26) Baltazar-Y-Jimenez, A.; Bismarck, A. *Cellulose* **2007**, *14*, 115–127.
- (27) Marquardt, D. W., *J. Soc. Ind. Appl. Math.* **1963**, *11*, 431.
- (28) Head, F. S. H. *J. Text. Inst.* **1958**, *49*, 345–356.
- (29) Schramm, C.; Rinderer, B. *Anal. Chem.* **2000**, *72*, 5829–5833.
- (30) Kullman, R. M. H.; Reinilardt, R. M. *Text. Res. J.* **1978**, *48*, 320–324.
- (31) Welch, C. M. *Text. Res. J.* **1983**, *53*, 181–186.
- (32) Meyer, U.; Muller, K.; Zollinger, H. *Text. Res. J.* **1976**, *46*, 756–762.
- (33) Reeves, W. A.; Drake, G. L.; McMillan, O. J.; Guthrie, J. D. *Text. Res. J.* **1955**, *25*, 41–46.
- (34) Krassig, H. *Papier* **1990**, *44*, 617–623.
- (35) Lee, E. S.; Kim, S. I. *Fibers Polym.* **2004**, *5*, 230–233.
- (36) Choi, H. M.; Kim, J. H.; Shin, S. *J. Appl. Polym. Sci.* **1999**, *73*, 2691–2699.
- (37) Gupta, K. C.; Jabrail, F. H. *Carbohydr. Res.* **2006**, *341*, 744–756.
- (38) McKenna, B. A.; Mikkelsen, D.; Wehr, J. B.; Gidley, M. J.; Menzies, N. W. *Cellulose* **2009**, *16*, 1047–1055.
- (39) Hamad, W. Y.; Eichhorn, S. *J. Eng. Mater. Technol.* **1997**, *119*, 309–313.
- (40) Eichhorn, S. J.; Hughes, M.; Snell, R.; Mott, L. *J. Mater. Sci. Lett.* **2000**, *19*, 721–723.
- (41) Rusli, R.; Shanmuganathan, K.; Rowan, S. J.; Weder, C.; Eichhorn, S. J. *Biomacromolecules* **2010**, *11*, 762–768.
- (42) Rusli, R.; Eichhorn, S. J. *Appl. Phys. Lett.* **2008**, *93*, 033111.
- (43) Gierlinger, N.; Schwanninger, M.; Reinecke, A.; Burgert, I. *Biomacromolecules* **2006**, *7*, 2077–2081.
- (44) Peetla, P.; Schenzel, K. C.; Diepenbrock, W. *Appl. Spectrosc.* **2006**, *60*, 682–691.
- (45) Wiley, J. H.; Atalla, R. H. *Carbohydr. Res.* **1987**, *160*, 113–129.
- (46) Edwards, H. G. M.; Farwell, D. W.; Webster, D. *Spectrochim. Acta, Part A* **1997**, *53*, 2383–2392.